Journal of Cleaner Production 19 (2011) 2066–2074

Contents lists available at ScienceDirect

Journal of Cleaner Production

journal homepage: www.elsevier.com/locate/jclepro

Shape memory polymer snap-fits for active disassembly

John Carrell [a], Derrick Tate [b], Shiren Wang [a,*], Hong-Chao Zhang [a,**]

[a] Department of Industrial Engineering, Texas Tech University, Lubbock, TX 79409-3061, USA
[b] Department of Mechanical Engineering, Texas Tech University, Lubbock, TX, USA

ARTICLE INFO

Article history:
Received 16 August 2010
Received in revised form
19 June 2011
Accepted 28 June 2011
Available online 12 July 2011

Keywords:
Active disassembly
Shape memory alloy
Taguchi methods
Shape memory polymer

ABSTRACT

This paper explores a means to simplify disassembly by engineering a snap-fit that automatically releases upon exposure to a heat field thus limiting manual labor or machine operation for disassembly. Shape memory polymer (SMP) snap-fits were designed and manufactured to actively release upon a thermal trigger. Snap-fits were designed with an added feature known here as a release angle that would allow for an uninterrupted movement for disassembly in the presence of an elevated temperature. SMP snap-fits were then manufactured and tested. Testing was performed for demonstration of the active release of the SMP snap-fits and for analysis of active disassembly (AD) process parameters. Taguchi methods were used to analyze the AD process parameters, including heating method and disassembly temperature. The results from this research show the successful demonstration of the SMP snap-fits within a manufactured product housing. AD process parameter analysis shows that both the heating method and temperature affect the AD process. The analysis determines that by increasing the heat exchange rate the snap-fit disassembly time is shortened. From the performed experiments, it was seen that an Oil bath at 150 °C produced the best results in regards to disassembly time and signal-noise ratio. The results from experimentation demonstrate the possibility of acceptable heat-releasable fasteners for more efficient disassembly and exhibit benefits over current AD elements comprised of shape memory alloys.

1. Introduction

With the current focus on the environment, disassembly is becoming a heavily promoted, if not mandatory, end-of-life (EoL) activity for many products because of the environmental benefits that can be gained by disassembly (Council Directive 2002/96/EC of 27 January 2003 on Waste Electrical and Electronic Equipment (WEEE), 2003). Disassembly can allow for the disposal of hazardous materials, increase component reuse, and provide purer recycling streams (Linton, 2000). Unfortunately, for a number of products, particularly small electronic products, disassembly has not been a popular EoL activity due mainly to the high cost of disassembly operations. Current disassembly operations are not economically viable and need to be improved in regards to labor, product integrity, and flexibility (Carrell et al., 2009). Disassembly operations in industry are done by either manual or automated methods. For manual disassembly, operators use tools to forcefully disassemble a large variety of products resulting in a large labor cost along with destruction of the product and its components. Automated disassembly is a more efficient method in regards to labor, but the product variety for automated disassembly is greatly limited and hardly justifies the investment in machinery (Duflou et al., 2008). Because of these deficiencies in current disassembly methods, research has continually focused on ways to improve the flexibility and efficiency of disassembly operations. Much of the focus has been on design methodologies that incorporate simple and efficient disassembly mechanisms. The most basic of these methodologies is Design for Disassembly (DfD) that relies on easily released fasteners within product assemblies, proper handling operations, and standardized designs for flexible and efficient disassembly operations (Zhang et al., 1997). The focus of DfD is on *one-to-one disassembly*, defined as one action releases one fastener. The one-to-one disassembly focus of DfD can make disassembly more efficient and flexible, but the benefits from DfD are limited according to the number of fastening elements within the design (Duflou et al., 2008). Because of this limitation, a concept of a *one-to-many disassembly process*, defined as one action releases a number of fasteners has been proposed. The one-to-many disassembly process has introduced two methodologies: Disassembly Embedded Design (DED) and Active Disassembly (AD). DED relies on specialized disassembly mechanisms within the product's

* Corresponding author.
** Corresponding author.
E-mail addresses: Shiren.Wang@ttu.edu (S. Wang), hong-chao.zhang@ttu.edu (H.-C. Zhang).

0959-6526/$ – see front matter © 2011 Elsevier Ltd. All rights reserved.
doi:10.1016/j.jclepro.2011.06.027

design. These specialized disassembly mechanisms will react to an environmental field (e.g. mechanical, thermal, chemical, etc.) and cause the product to disassemble. Conceptual designs for DED have shown efficiency improvements with disassembly processes, but due to their specialization per product, intense work in the design stage is needed, which limits DED's flexibility and use (Willems et al., 2005). In an effort to reduce this design work and increase flexibility, AD has resulted. Unlike DED, AD relies on generic fastening elements, which can be easily incorporated into existing designs with little to no added design effort. This general application of such elements has created the flexible and efficient disassembly processes needed to make disassembly a more economically viable EoL activity (Duflou et al.,2006).

A number of AD elements have been conceptually designed and analyzed. A good review of basic AD concepts can be seen in Duflou, Willems et al. (Duflou et al.,2006), where the mechanisms for freezing elements, pneumo-elements, soluble elements, and shape memory material (SMM) elements are all analyzed and critiqued. Beyond conceptual review, more in-depth discussion and modeling of elements has been seen with hydrogen-storage alloys and pressure-triggered elements. Kasa and Suga (Kasa and Suga, 1999), Suga (Suga, 1999), and Suga and Hosada (Suga and Hosoda, 2000) provide an in-depth analysis of hydrogen-storage alloys, which are special alloys that can bond surfaces together. When exposed to a high-hydrogen environment, these alloys break down releasing the bond. The focus for hydrogen-storage alloys has been in the disassembly of bonded integrated circuits in printed circuit boards. Willems, Dewulf et al.(Willems et al., 2007a,b) used topology modeling to design and analyze a pressure-triggered element. Design of the element was based on a plastic assembly snap that would release and separate product components at increased pressures (Willems et al., 2007a,b).

While these studies provide conceptual examples of how AD can be incorporated within product designs, only a few studies have actually designed, manufactured, and tested AD elements. Of these studies, the Cleaner Research group at Brunel University in England has performed the most research. The Cleaner Research group has primarily focused on SMM elements. Their first studies started with shape memory alloys (SMAs), which recover large stress deformations when heated above their martensitic transformation temperature. Because the deformation is stress induced, SMAs exhibit large forces during their recovery or shape memory effect (SME) (Otsuka and Wayman, 1998). With this in mind, the Cleaner Research group retrofitted a variety of electronic devices with SMA actuators that force open a product assembly upon exposure to a thermal field. The results from these studies showed the flexibility and effectiveness through the successful implementation of the SMA actuators for disassembly of electronic products (Chiodo et al., 1997, Chiodo et al., 1998a,b, 2002).

Another set of AD studies performed by the Cleaner Research group involved shape memory polymers (SMPs). SMPs are similar to SMAs as their SME is heat-activated, but the mechanism for the SME is mainly strained based meaning they do not exhibit large recovery forces. This has made them more suitable for releasable fasteners (Chiodo et al., 1998a,b). The first study using SMP elements was seen in Chiodo et al., inpress, (Chiodo et al., 1998a,b), where a SMP compression sleeve was designed and implemented to release an assembly bolt. The group continued its study with SMPs with the design of SMP screws. At ambient temperatures, the SMP screws function like regular screws, and at elevated temperatures, the screws lose their threading to release from the product. Retrofitting of these screws has been done in a number of AD studies for electronic products (Chiodo et al., 1999a,b; Chiodo et al.,inpress). Beyond retrofitting with SMP compression sleeves screws, the Cleaner Research group has also looked at original element designs for specific product applications, such as an LCD bracket that will release upon a thermal trigger (Chiodo et al., 2000).

The purpose of this research was to expand on previous works in AD by designing, manufacturing, and testing a SMP heat-releasable snap-fit. In doing so, two main objectives were determined that could differentiate this research from previous works. These objectives included:

- Create a generic design and application of heat-releasable SMP snap-fits. The snap-fit is a very common fastener and by using it as the foundation for a heat-releasable SMP snap-fit the makes the incorporation of the SMP snap-fit within existing products simple. This simple application would not require efforts for retrofitting as with previous works particularly with SMA elements and some SMP elements
- Determine AD control parameter analysis. A detailed analysis of the heating method and temperature for the snap-fits were determined by testing. This provided key data into how the AD process should be controlled and goes beyond the pass/fail disassembly criteria in previous works

This paper will further discuss the methods for meeting these objectives by first discussing the special shape memory properties and mechanism of SMPs that affected the design of the SMP along with accepted models for the shape recovery of the SMP to explain the heat recovery of the SMP snap-fit. Establishment of experiment procedures will then be made along with the results of such experiments. Finally, a discussion will be made to compare the desired objectives with actual results seen in experimentation.

2. Methods

2.1. SMP mechanism

SMPs have the ability to hold and recover temporary deformations upon application of a heat field. This special ability is based on the SME of the SMP, which is explained by the material behavior of the SMP at various thermal and mechanical constraints (Gall et al., 2002; Sittner et al., 2002). The basis of the SME is on the polymer architecture, which consists of special "switching" and "hard" segment cross-links. The hard segment cross-links set the permanent shape of the polymer and are the strong cross-links formed by chemical bonding. Conversely, the switching segment cross-links are reversible cross-links that upon heating to the glass transition temperature (T_g) allow the SMP to be deformed in an open state and set into a secondary shape in a closed state. The thermo-mechanical mechanism for the SME is illustrated in Fig. 1. From Fig. 1, State A shows the SMP heated above the T_g. Above the T_g, the switching segments are in a state of hyperelasticity, and the hard segment cross-links hold the polymer in its permanent shape. Because the switching segments are hyperelastic, the SMP is in a rubbery state allowing for easy deformation, seen from State B. In State B, the deformations set the SMP into the desired secondary shape and based on the drastically reduced mechanical properties (i.e. tensile strength, elastic modulus, etc.) the needed deformation stress is minimal. Cooling the polymer under constraint, as seen in State C, will allow those switching segments to "turn on" or return to a rigid state. These switching segments would then hold the deformation and place the SMP is in its glassy state, as seen in State *D*. Reheating the SMP would then return the switching segments to a hyperelastic state and allow the hard segment cross-links to return to their position thus returning the SMP back to its permanent shape, seen in State A (Otsuka and Wayman, 1998; Liu et al., 2007; Behl and Lendlein, 2007).

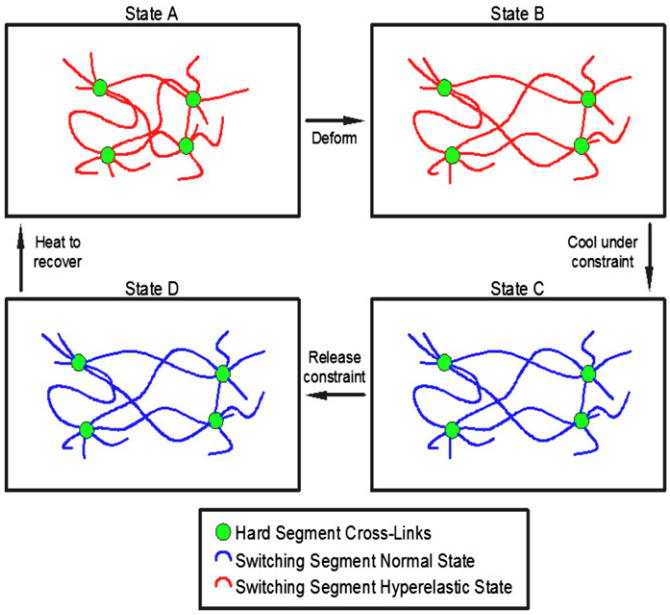

Fig. 1. Illustration of SME in SMP network-adapted from Behl and Lendlein (Behl and Lendlein, 2007).

Understanding the shape memory properties of the SMP was important in explaining the heat actuation and relating results from the performed experiments. Of particular interest in this research was the actuation time for shape recovery of the SMP snap-fits. In considering this performance characteristic previous models for shape memory behavior were used to explain the key variables and findings in this research. For the intent of this research, a previously developed storage deformation model (See Liu et al (Liu et al., 2006)) was used. Storage deformation models separate the transition phases of the SMP into two phases: an active phase and frozen phase. The active phase is the rubbery state of the SMP, where conformational change of the macromolecular chain is allowed and deformation is entropic. The frozen phase is the rigid state of the SMP, where conformational change is stored and the deformation entropic energy is internal energy. These models assume a change in volume fraction of the SMP from rigid material to rubbery material or vice-versa at given temperatures. Commonly, the Helmholtz energy explains this relationship,

$$H_{\text{total}} = f_r(T)H_r + f_g(T)H_g \tag{1}$$

where H_{total} is the total Helmholtz energy at temperature T, $H_r$is the Helmholtz energy of the rubbery material at $T > T_g$, H_g, is the Helmholtz energy of the glassy material at $T \ll T_g$, f_r, and f_g are thus functions of temperature and their sum must be equal to 1. Likewise, equations for stress and strain can be developed,

$$\begin{aligned} \epsilon &= f_f\epsilon_f + \left(1 - f_f\right)\epsilon_a \\ \sigma &= f_f\sigma_f + \left(1 - f_f\right)\sigma_a \end{aligned} \tag{2}$$

where:σ and ϵ are the total stress and strain, σ_f and ϵ_f are the stress and strain of the frozen phase, σ_a and ϵ_a are the stress and strain of the rubbery phase, and f_f the volume fraction of the frozen phase, which is derived by

$$f_f = 1 - \frac{1}{1 + c_f(T_h - T)^n} \tag{3}$$

where: T_h is the reference temperature, c_f and n are thermal fitting.

The storage deformation energy and thus strain is present during the frozen and active phase. These strains are key for the modeling the SME. The frozen strain, which is the strain following cooling and trained deformation, is modeled by

$$\epsilon_f = \int^{f_f} \epsilon_f^e(x)\mathrm{d}f + \epsilon_f^i + \epsilon_f^T \tag{4}$$

where: ϵ_f^e is the entropic frozen strain, ϵ_f^i is the internal energetic strain and ϵ_f^T is the frozen thermal strain. ϵ_f^e can be anisotropic and should thus be integrated with respect to position vector, x, to determine the overall contribution.

The stored strained in the frozen state explains the end state for the polymer (i.e. trained, set deformation), but the thermal process (i.e. the cooling to store and heating to recover) effectively stores strain, as well and must also be accounted for to explain the SME. This strain explains the active strain,

$$\epsilon_a = \epsilon_a^e + \epsilon_a^T \tag{5}$$

where: ϵ_a^e is the entropic active strain and ϵ_a^T is the active thermal strain. In combination of the two strains, the total strain during any period in the thermomechanical cycle becomes

$$\epsilon = \int^{f_f} \epsilon_f^e(x)\mathrm{d}f + \left[f_f\epsilon_f^i + \left(1 - f_f\right)\epsilon_a^e\right] + \left[f_f\epsilon_f^T + \left(1 - f_f\right)\epsilon_a^T\right] \tag{6}$$

This strain model would build upon the shape recovery rate of the SMP by considering the heat transfer to the SMP. Respectfully, full recovery is seen when the active phase volume is 100%, and it is then safe to assume that this active phase can only be reached when the entire SMP part is above. Particularly, Eq. (4) points out the thermal fitting parameters for the SMP that correspond to the volume fraction of the SMP and are thus dependent on the thermal properties of the SMPs. The recovery rate can be modeled according to the heat transfer by using Fourier's law. A simple model for the heat transfer between the heating body and the part can be calculated by determining

$$t = -T\ln\frac{T_\infty - T_g}{T_\infty - T_i} \tag{7}$$

where T is a time constant for the part, $T_i$is the initial temperature of the part, $T\infty$ is the temperature of the heating body, t time to heat the part to its is the glass transition temperature (T_g). The time constant T will thus be dependent on the heat transfer coefficient between the part and the heating body via

$$T = \frac{\rho cV}{\bar{h}A} \tag{8}$$

where ρ is the density of the part, c is the specific heat capacity of the part, V is volume of the part, $\bar{h}$ is the heat transfer coefficient between the part and the heating body, and is the heating area of the part (Lienhard, 2008).

Based on the strain model and time response model, the shape recovery was determined to be dependent on the density of the SMP, heat capacity of the SMP, volume of the SMP part, heat transfer between the SMP part and heating body, and the residual storage deformation strain. These variables were therefore the main factors that affect the actuation for shape recovery of the SMP elements in the AD process. Furthermore, these variables also showed the importance in the design of the SMP element in shape recovery and actuation.

2.2. Snap fit design

Considering the SMP's SME, the design of the SMP snap-fit followed criteria based on 1) the need for both a permanent and temporary shape and 2) the limited mechanical properties for recovery. The SMP requires two shapes. One shape will be the permanent shape of the SMP and will be the return shape upon heating the unconstrained SMP. Since a heat-activated disassembly action was desired for the snap-fit the permanent shape was determined to be the release shape of the SMP. The other shape was the temporary shape of the SMP for which the SMP returns from upon heating. It was then desired that the temporary shape be the normal shape of a snap-fit.

This release shape is dependent on the mechanical properties of the SMP for shape recovery. The limited mechanical properties for recovery are explained by the internal forces of the hard segments to return to their primary position and are the main drivers in the shape recovery the key component to the recovery stress of the SMP. Typically, the recovery stress is very small, and even upon small force constraints, shape recovery can be greatly hindered. The design of the SMP element thus becomes important for proper shape recovery. The design of the snap-fit in this case must be so that unnecessary constraints are avoided in shape recovery. For the snap-fit, this is done by the release angle of the snap-fit and fixed section at the end of the snap-fit. The release angle and fixed section will create a rotating motion about the fixed section. This rotation is essential to avoid constraints upon the snap-fit (See Fig. 2). The surface contact between snap-fit and the housing catch will create friction once the snap-fit begins its release. By rotating about the fix section of the snap-fit this contact is reduced at the beginning of the movement of the snap-fit and allows for unconstrained recovery of the snap-fit. The rotation is mitigated by the added pressure due to thermal expansion of the snap-fit and housing catch.

3. Experiment

3.1. Active disassembly experiments

SMP snap-fits were designed and manufactured for experimentation. The design of the snap-fits called for consideration of a primary shape and secondary shape. The primary shape of the snap-fit was the return shape of the snap-fit upon heat activation. The primary shape thus required an added release angle that would determine the deflection of the snap-fit upon heat actuation (See Fig. 3). The snap-fits were machined *according this primary shape design from a sheet* 6.35 mm *commercially available SMP thermosetting known as Veriflex. Veriflex* is a two-part epoxy that is produced by Cornerstone Research Group Inc. To perform the necessary deflection upon heat actuation, the snap-fits were programmed or trained into a secondary shape. The secondary shape for the snap-fit straightened the snap-fit for assembly. This secondary shape is the common shape of regular polymer snap-fits. The training process was accomplished by a combination of thermal and mechanical fields. Above its T_g, the Veriflex is very pliable and can thus be easily formed or trained into a secondary shape. Holding the secondary shape and cooling the snap-fits below the T_g sets the secondary shape, and upon unconstrained reheating will allow the return of the snap-fit to its primary shape (See Fig. 4).

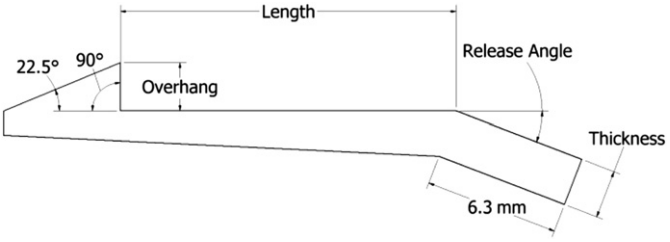

Fig. 3. Designed Snap-Fit. Set parameters are listed and variable parameters seen in Table 2.

The intent of this research was to demonstrate SMP snap-fits for heat-activated disassembly. In doing this an object needed to be disassembled, so simple housings to which the snap-fits would hold together and upon heat activation disassemble were machined. PC was chosen as the housing material because of its thermal properties (Vicat Softening Point ~150 °C) that could

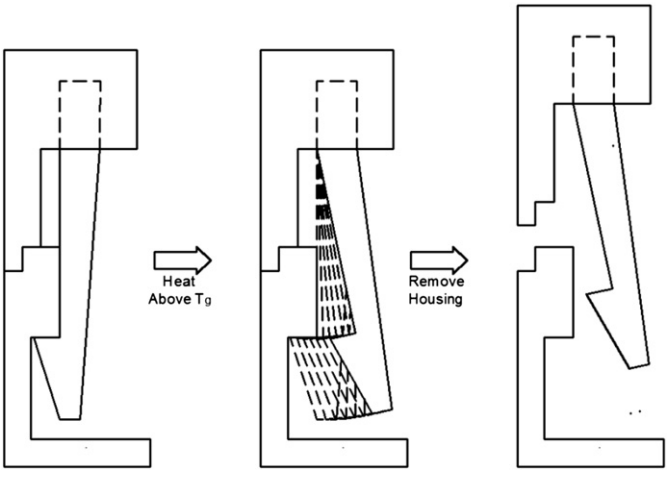

Fig. 2. Heat activated release of SMP snap-fit and housing removal.

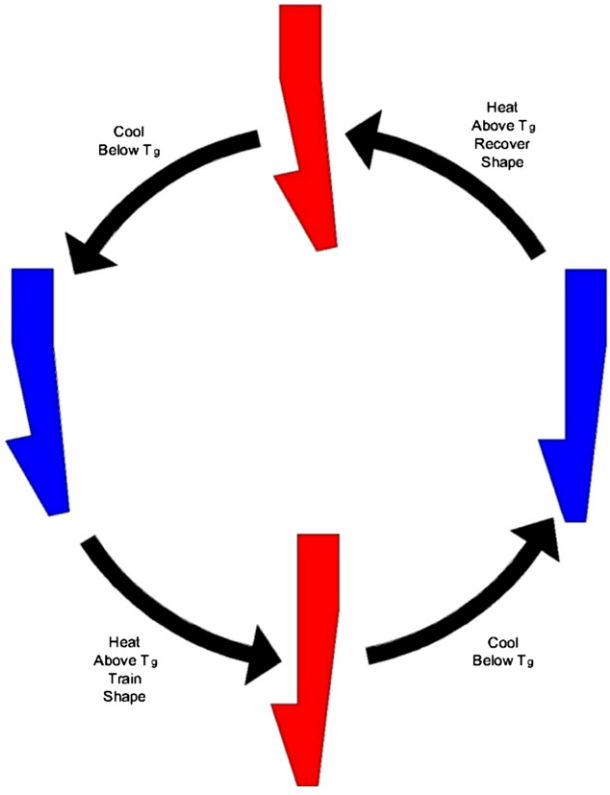

Fig. 4. Thermomechanical Cycle for SMP Snap-Fit.

Table 1
Control and Noise Factors and Levels.

Factor	Levels			
	1	2	3	4
A. Method	Air	Oil	–	–
B. Temperature	130 °C	140 °C	150 °C	–
C. Design	1	2	3	4

Table 2
Snap-Fit design parameters.

Design	Length (mm)	Overhang (mm)	Thickness (mm)	Release angle (°)
1	15.9	2.3	2.3	159
2	15.9	1.5	1.8	167
3	12.7	2.3	1.8	153
4	12.7	1.5	2.3	163

Note: Per the design constraints, the assembly angle, disassembly angle, and width were constant at 45°, 90°, and 6.35 mm, respectively.

withstand the thermal cycling of the snap-fits for heat actuation. PC is also naturally transparent, which permitted the release of the snap-fit to be seen through the housing. The pieces for the PC housings were machined according to the dimensions of the SMP snap-fits. Top and bottom housings were assembled using screws. Screws were also used to affix the assembly tab of the snap-fits within the top housings. Once the snap-fits were attached, the housings were assembled by latching the snap-fit of the top housings to the recess in the bottom housing.

Designed experiments were performed to determine the key control factors for the AD process. Taguchi methods were incorporated in this set of experiments (Phadke, 1989). Control factors for the AD process included the method of heating (Oil bath or Air bath) and the temperature for disassembly. Based on trial experiments, the temperatures levels were chosen to be 130 °C, 140 °C, and 150 °C. Noise factors of interest were the variable dimensions of the snap-fits (See Table 1). In an industrialized AD process, it is expected that a variety of products will be processed. With a variety of products process, it would be difficult to control the design of snap-fits within each product thus making the design of the snap-fit an uncontrollable noise factor. For the experiment, the noise due to design was simulated by testing the four designs of the snap-fit (See Table 2). For Air bath testing, assembled housings were placed in a Fisher.

Isotemp Gravity Convection Oven and were allowed to dwell at temperature until release of all the snap-fits was seen. For Oil bath testing, assembled housings were placed in a Buchi Heating Bath. Since temperature control was done manually, a ±5 °C allowance from the set temperature was made for both Air and Oil bath testing.

Because the disassembly time effectively measures the efficiency and effectiveness of the AD process, it was chosen as the quality characteristic or measured response for this research. To account for the noise and variability within the process, a signal-to-noise ratio was created for the disassembly time. The signal-to-noise ratio measured the control the temperature and heating method have over the disassembly time with the inherent noise or variability of the AD process. A maximum value in the signal-to-noise ratio indicated the disassembly process that minimizes the time for disassembly while also minimizing the noise or variability in the process. The signal-noise ratio was thus based on a smaller-the-better type,

$$\eta = -10\log_{10}\left(\frac{1}{n}\sum_{i=1}^{n} y_i^2\right) \tag{9}$$

where: η is the Signal-to-noise ratio, n is the number of responses, and y_i is the response for the *ith* response.

3.2. Shape memory testing experiments

In concurrence with the anticipated results for active release of the SMP snap-fits under application of a heat field, basic shape memory testing was also performed. This basic testing was performed in a Shimadzu AGS J Tensile Test machine fitted with a thermal chamber. Column shaped Veriflex samples (45 mm L × 2.5 W × 8.5 mm) were machined and tested using the following procedure:

1. Verifelx samples heated above T_g (105 °C according to ref (Veriflex E2 Epoxy, 2009)) and stretched to 44% strain. Resulting stress-strain was recorded
2. Veriflex samples while constrained in machine were allowed to cool to room temperature.
3. Bottom constraint of Veriflex sample was removed and Veriflex sample. Resulting strain was measured. Shape fixity of the Veriflex was determined according to this step by:

$$R_f = \frac{\epsilon_m - \epsilon_p}{\epsilon_m}$$

4. While unconstrained Veriflex sample was heated above T_g for shape recovery and allowed to cool. Resulting strain was measured. Shape recovery was determined according to this step by:

$$R_r = \frac{\epsilon_0 - \epsilon_p}{\epsilon_0}$$

Along with thermomechanical shape memory testing, a basic tensile test was also performed on the Veriflex at room

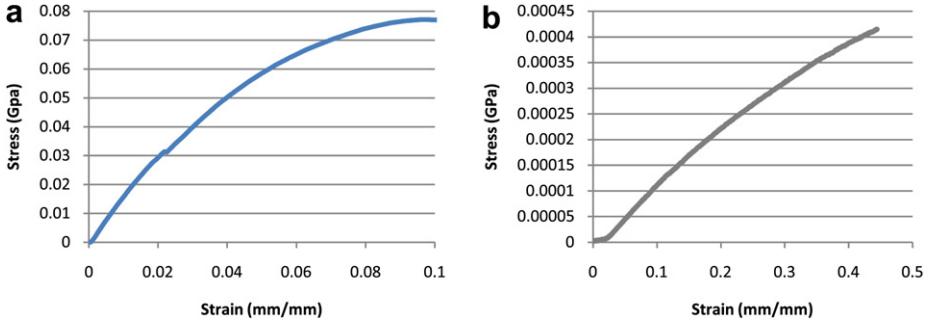

Fig. 5. Tensile Test Results, a) results for Veriflex at room temperature and b) results for Veriflex at 105 °C.

Table 3
Shape memory testing results.

Sample	Original length (mm)	Stretched length (mm)	Recovered length (mm)	Fixity (%)	Recovery (%)
1	45.90	63.36	45.85	96.19%	99.89%
2	46.22	63.46	45.90	96.27%	99.30%
3	44.89	62.73	44.87	96.68%	99.96%

temperature. This analysis provided key mechanical property differences for the SMP at room temperature and elevated temperatures.

4. Results

4.1. Shape memory testing results

Tensile testing of the Veriflex was performed at room temperature (~25 °C) and at an elevated temperature above the T_g (~105 °C). The results of this test show a drastic change in mechanical properties of the Veriflex above the T_g. At room temperature, the modulus is approximately 1.536 GPa and acts as a normal epoxy would. Above T_g, the modulus drastically drops to approximately 0.01120 GPa and can be easily deformed. These results are presented in Fig. 5.

Shape memory testing results shows good shape recovery and fixity for the Veriflex making the Veriflex a good candidate for the actively releasable snap-fit fasteners (See Table 3). Average fixity of the Veriflex is approximately 96% and average recovery is approximately 99%. These values would indicate a great ability for the Veriflex to be trained in a particular shape and recover that shape upon heating above T_g.

4.2. Active disassembly testing results

The SMP snap-fits were all successfully actuated by a heat field in testing and allowed for easy separation of the manufactured housings (See Fig. 6). Results from the designed experiments are seen in Table 4. In this table the experiments are grouped according to method and temperature. For each scenario of method and temperature, the average, standard deviation, and signal-noise ratio are calculated.

The shortest time for disassembly from the experiments occurred with Design 3 when it was placed in an Oil bath at 150 °C where a disassembly time of 0.742 min was seen. The longest disassembly time was for Design 4 in an Air bath at 130 °C. Along with these extreme cases, a number of trends are present in Table 3. There is a significant decrease in average disassembly times between an Air and Oil bath. The use of an Oil bath for decreased average disassembly time tends to agree with past research (Liu et al., 2007; Lendlein and Kelch, 2002; Hussein and Harrison, 2008). The cause of this decrease is the higher heat capacity the oil has over air increasing the rate of heat exchange to the snap-fits. To go along with this decrease in average disassembly time, a decrease in standard deviation from an Air to Oil bath is also seen. Increasing the temperature will also reduce the disassembly time. Again by increasing the temperature an increase in heat transfer rate is seen explaining the decrease in disassembly time. The standard deviation also decreases with an increase in temperature, but this decrease is not as pronounced as with the heating method.

As previously stated, in analyzing the signal-noise ratios the focus is put on maximizing the value. The signal-noise ratios are linked to the average disassembly times from Table 3 and show the same basic trends. From Fig. 7, by choosing an Oil bath over an Air bath, the signal-noise ratio significantly increases. An increase in signal-noise ratio is also seen with an increase in temperature, but this increase is not as significant when compared the heating method. Overall, the minimum signal-noise ratio is seen with an Air bath at 130 °C, and the maximum signal-noise ratio is seen with an Oil bath at 150 °C.

The interaction between the heating method and temperature, seen in Fig. 8, compounds the results from the factor-by-factor analysis. The highest signal-noise ratios are seen with an Oil bath, which are well above any signal-noise ratios for an Air bath. By increasing the temperature with an Oil bath, the signal-noise ratios appear to constantly increase and would seem to continue to increase above the 150 °C threshold from this research. For an Air bath, this does not appear to be the case. The signal-noise ratios increase with temperature, but it does appear that the signal-noise ratio might level off shortly after exceeding 150 °C.

The ANOVA analysis verifies the main effects to the signal-noise ratios according to the heating method and temperature. From the ANOVA table (See Table 5), much of the variance can be attributed to the heating method, which accounts for 96.7% of the total sum of squares. The temperature only accounts for 4.25% of the total sum of squares. While the temperature accounts for a minimal amount of the sum of squares and could be attributed to the natural error in the experiment, hypothesis testing can provide statistical evidence that the temperature does affect the AD process. By assuming a Type 1 error of 5%, the F-test statistics for both the heating method and temperature both show that they affect the signal-noise ratio for the AD process.

5. Discussion

The experiments performed provide a good example of the effectiveness of the SMP as a viable heat-activated releasable fastener for active disassembly. The application of the SMP snap-fits could easily be altered to be used in a number of existing product designs. This is due to the generic design of the SMP snap-fit, which is based on existing snap-fit designs, but with an additional release angle feature due to its shape recovery ability. This generality of the SMP snap-fit makes it a more viable option than other AD elements, particularly SMA elements, because of the possible incorporation within the existing product design. Due to their force exertion

Fig. 6. Disassembly process, a) assembled housing with latched snap-fits, b) enclosed housing after heating and dwelling at transition temperature, c) separation of housings.

Table 4
Summary of experiment results.

Method	Temp	Design				Average	Std. Dev.	S/N
		1	2	3	4			
Air	130 °C	13.477	11.811	14.523	15.372	13.796	1.533	−22.835
Air	140 °C	9.045	7.545	9.639	9.645	8.969	0.990	−19.094
Air	150 °C	7.823	7.476	7.601	9.457	8.089	0.923	−18.200
Oil	130 °C	1.845	1.159	1.123	1.435	1.391	0.334	−3.047
Oil	140 °C	1.015	0.835	0.929	1.122	0.975	0.122	0.167
Oil	150 °C	0.777	0.745	0.742	0.796	0.765	0.026	2.323

during shape recovery SMA elements are used to force components in AD products, but the problem that arises in such an application is the focus on placement of the SMA element. If the SMA element is not place properly heat-activated disassembly can fail and can even damage the product (Chiodo et al., 2002). Because the SMP snap-fit can be easily incorporated within the product with the replacement of existing snap-fits, placement is not an issue and does not hinder the design process. While placement of the SMP snap-fit is not an issue, the design of the SMP snap-fit and catch within the product could possibly present issues where heat-activated disassembly can fail. Failure could be possible with cases of great thermal expansion of the housing catch and SMP snap-fit, which would impede the shape recovery force of the SMP. This was not a problem in experimentation due to the design of the snap-fit and catch along with the selected materials for the experiment, which have relatively low thermal expansion stress in comparison to the recovery stress of the Veriflex. A detailed analysis of recovery stress for the Veriflex is seen in Tandon et al (Tandon et al., 2009). In this work, the Veriflex exhibits sustained recovery stress of approximately 0.56 MPa and momentary maximum recovery stress of approximately 0.76 MPa. Given these recovery stress values, there should be sufficient recovery force to allow for a number of heat-releasable snap-fit designs to disassemble easily upon heat activation. If, however, heat-activated release is inhibited by the special design of other products, the flexibility in design of the SMP snap-fit, particularly in the permanent shape, could alleviate this problem. For example, Fig. 9 illustrates such a primary shape for the snap-fit, which is similar to the MPL SMP screws seen in Chiodo et al., inpress (Chiodo et al., 1999a,b). This snap-fit overhang would be formed in training. Upon heat recovery the overhang of the snap-fit will pull away from the surface of the housing catch and the snap-fit would elongate. This would avoid any surface friction force constraints and simple part separation could follow. This flexibility in design of the permanent shape of the SMP snap-fit provides another benefit over other SMA elements and again puts a focus on design of the product (i.e. snap-fit and catch) rather than placement.

Thermomechanical properties of the SMP also exhibit a particular benefit over SMAs in the training process. The most striking being the drastic change in modulus for the SMP above T_g. This mechanical change provides a clear benefit of SMPs over SMAs in shape training because little force is needed to form the SMP into its secondary shape which is done above. SMAs do not exhibit the drastic drop in modulus with heating and require a large force to shape into its secondary shape (Meng and Hu, 2009). Furthermore, the shape recovery exhibited by SMPs is much greater than SMAs. As exhibited in this research, approximately 44% strain was recovered by the SMP in the testing performed in this research and greater strains (up to 800%) could be recovered barring limitations of the tensile machine fitted with the thermal chamber. SMAs have been limited by their secondary shape to deformations of approximately 8% strain (Liu et al., 2007).

Flexibility with the AD process is also seen with temperature controls and applied heating methods per the experimental results. The results from experimentation match the emphasis on increased heat transfer to reduce recovery time from the accepted models. As previously established, the shape recovery of the snap-fits is dependent on the density of the SMP, heat capacity of the SMP, volume of the SMP part, and heat transfer between the SMP part and heating body, and the residual storage deformation strain. For the experiment, the SMP density and heat capacity are constant for the snap-fits, so the design of the snap-fit and heat transfer coefficient become the main controlling factors for the heating process and shape recovery. In the performed experiments, the designs of the snap-fits were varied and the resulting varied volumes, surface areas, and residual storage deformation strains explain the slight differences in recovery rates at tested temperatures. The results show this but due to the small changes in design drastic changes in the shape recovery rate was not seen. This could not be said for the

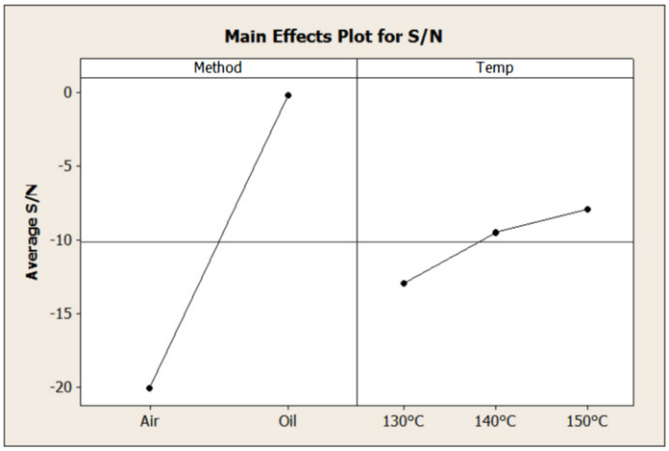

Fig. 7. Main Effects Plot for Signal-Noise ratios.

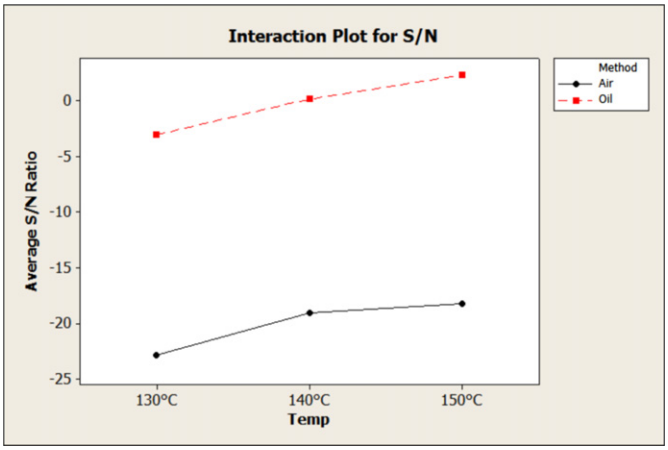

Fig. 8. Interaction Plot for Signal-Noise ratio.

Table 5
ANOVA table for S/N ratio.

Factor	Average S/N by level			Degrees of freedom	Sum of squares	Mean sum of squares
	1	2	3			
Method	−20.043	−0.186	–	1	591.471	591.471
Temperature	−12.941	−9.464	−7.939	2	26.296	13.148
Error				2	0.402	0.201
Total				5	618.168	

Note: Overall mean $\eta = -10.115$. For Method, Level 1 and 2 correspond to Air and Oil Bath. For Temperature, Level 1, 2, and 3 correspond to 130 °C, 140 °C, 150 °C.

heat transfer coefficient, which is the main contributor to the change in shape recovery rates. The heat transfer coefficient is a complex variable and was not explicitly determined in this research, but considering past research works the heat transfer coefficients can change by an order of magnitude from gases to liquids. There is variability due to the added housing, which can impede the heat transfer to the SMP snap-fit and thus increase the time for recovery. This is particularly evident in comparison to other SMP shape recovery tests, where the recovery was seen in a matter of seconds (Chiodo et al., 1999a,b). Even with such an impediment on the shape recovery time with the SMP snap-fits, the actual AD process can be altered by batching products together for disassembly. This in turn can greatly reduce the per product disassembly time and exceed cases where manual disassembly is less than the shape recovery time of the SMP snap-fit.

For example, consider the manual disassembly analysis of (See Table 6 and Fig. 10). From this analysis, there is very little value in recycling such small components, especially in lieu of the cost to disassemble. However, if the cost for disassembly can be reduced then recycling of these products may be more economically feasible. If the product is set with AD elements such as the studied

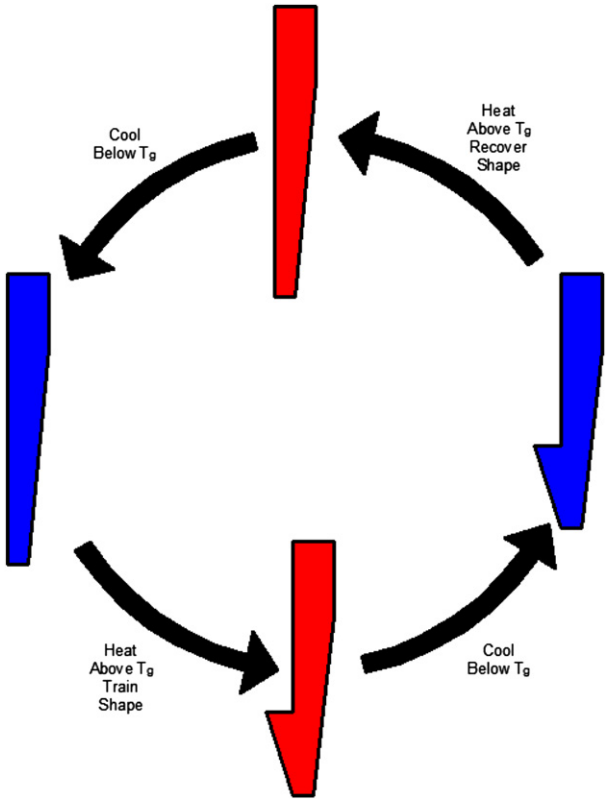

Fig. 9. Possible configuration for mitigating excess force constraints due to surface friction.

Table 6
Disassembly analysis for Siemens 4100 SpeedStream DSL modem.

Step	Element	Component(s) removed			
		Name	Weight (g)	Material	Time
1	Remove feet (4)	Feet (2)	0.29	Rubber	0.049
2	Remove housing screws (1)	Housing Screw	0.46	Steel	0.094
3	Press snap fits housing. separate housing	Top Housing	35.42	ABS	0.135
		Front Plate	2.84	PC	
		Light Board	0.85	PC	
4	Lift and remove PCB	PCB	70.27	PCB	0.038
		Bottom Housing	37.76	ABS	
Total					0.317

Fig. 10. Siemens 4100 SpeedStream DSL Modem.

SMP snap-fits and previously explained SMP screws, the manual disassembly time will still be much less than the anticipated AD times and would not appear to be beneficial for disassembly (Chiodo et al., 1999a,b). However, what is not evident in this analysis would be the ability for the AD product to be batched for disassembly processing. Many AD products could be batched and placed in an oil bath for heating and subsequent disassembly. If the heat actuation time for the AD elements is assumed to be 1.500 min (a conservative estimate) then a minimum batch size of 5 could reduce the per product disassembly time. An increase of the batch size would show even greater reductions in the per product disassembly times and increase the disassembly process.

6. Conclusion

This paper demonstrates an effective method to make the disassembly process more efficient with the integration of engineering SMP snap-fits that release upon application of a heat field. Based on this demonstration, limited manual or machine operation will be needed to disassembly product assemblies with these SMP snap-fits. This establishes AD as a more efficient option for disassembly through the ability to batch products for treatment. Batching with AD replaces the traditional one-at-a-time manual disassembly processing. This opens the case for disassembly in more products at end-of-life. Particularly, AD would be most applicable in increasing the number of small electronic products for end-of-life disassembly. Currently, the disassembly benefits (i.e. material recovery and hazardous material removal) of these small products do not overcome the burden of the current disassembly process and are thus not disassembled at end-of-life.

Also demonstrated in this research is basic shape memory properties of the SMP used for testing. These tests illustrate the usefulness of the SMP for AD by demonstrating the ability of the SMP to be successfully trained in a temporary shape and to be returned to an original shape with an applied heat field. Furthermore, the flexibility of the shape memory fixity and recovery of the SMP show a simple incorporation of these fasteners within existing designs and for new designs, which is an added benefit over other retrofitting SMA elements.

Along with this demonstration, process parameters for the AD process were analyzed. Results of this analysis show the AD process is controllable per the heating method and temperature. The basis of the control of the AD process is through the heat transfer to and the heat capacity of the SMP snap-fits, which has been established by a prior model (Liu et al., 2006). This explains the reasons that the disassembly efficiency is dependent on the process condition, such as heating temperature and method. The results illustrate that with an increase in heat transfer particularly through oil immersion a large decrease in the actuation time of the SMP will be seen. Also, an increase in temperature will decrease the actuation time of the SMP. These results provide the best conditions occurring with an oil bath at 150 °C.

Acknowledgments

The authors would like to gratefully acknowledge financial support from the Advance Manufacturing Laboratory at Texas Tech University and the Texas Tech Industrial Engineering Department. The support from Texas Tech Summer Dissertation Award is also acknowledged.

References

Behl, M., Lendlein, A., 2007. Shape-memory polymers. Materials Today 10 (4), 20–28.
Carrell, J., Zhang, H.-C., Tate, D., Li, H., 2009. Review and future of active disassembly. International Journal of Sustainable Engineering 2 (4), 252–264.
inpress Chiodo J.D., Billett E.H., Harrison D.J., Preliminary investigations of active disassembly using shape memory polymers. Environmentally Conscious Design and Inverse Manufacturing, 1999 Proceedings Eco Design '99: First International Symposium On 1999. pp. 590–596.
Chiodo, J., Anson, A., Billett, E., Harrison, D., Perkins, M., 1997. Eco-Design for Active Disassembly using Smart Materials. International Conference on Shape Memory and Superelastic Technologies. Pacific Grove, California, USA 269–74.
Chiodo, J.D., Billett, E.H., Harrison, D.J., Harry, P., 1998a. Investigations of Generic Self Disassembly using Shape Memory Alloys. IEEE International Symposium on Electronics and the Environment. 82–87.
Chiodo, J., Billet, E., Harrison, D., 1998b. Active disassembly. Journal of Sustainable Product Design 7, 26–36.
Chiodo, J.D., Billett, E.H., Harrison, D.J., 1999a. Active Disassembly using Shape Memory Polymers for the Mobile Phone Industry. IEEE International Symposium on Electronics and the Environment. 151–156.
Chiodo, J.D., Billett, E.H., Harrison, D.J., 1999b. Preliminary investigations of active disassembly using shape memory polymers. EcoDesign '99: First International Symposium On Environmentally Conscious Design and Inverse Manufacturing 590–596.
Chiodo, J.D., McLaren, J., Billett, E.H., Harrison, D.J., 2000. Isolating LCD's at End-of-Life using Active Disassembly Technology: A Feasibility Study. IEEE International Symposium on Electronics and the Environment. 318–23.
Chiodo, J.D., Jones, N., Billett, E.H., Harrison, D.J., 2002. Shape memory alloy actuators for active disassembly using 'smart' materials of consumer electronic products. Materials and Design 23 (5), 471–478.
EU, 2003. Council Directive 2002/96/EC of 27 January 2003 on Waste Electrical and Electronic Equipment (WEEE).
Duflou, J.R., Willems, B., Dewulf, W., 2006. Towards self-disassembling products Design solutions for economically feasible large-scale disassembly. Innovation in Life Cycle Engineering and Sustainable Development, 87–110.
Duflou, J.R., Seliger, G., Kara, S., Umeda, Y., Ometto, A., Willems, B., 2008. Efficiency and feasibility of product disassembly: a case-based study. CIRP Annals – Manufacturing Technology 57 (2), 583–600.
Gall, K., Dunn, M.L., Liu, Y., Finch, D., Lake, M., Munshi, N.A., 2002. Shape memory polymer nanocomposites. Acta Materialia 50 (20), 5115–5126.
Hussein, H., Harrison, D., 2008. New technologies for active disassembly: using the shape memory effect in engineering polymers. International Journal of Product Development 6 (3–4), 431–449.
Kasa D., Suga T., Active disassembly of bonded wafers. First International Symposium on Environmentally Conscious Degign and Inverse Manufacturing, Proceedings. 1999:pp. 588–589.
Lendlein, A., Kelch, S., 2002. Shape-Memory polymers %. Journal of Angewandte Chemie International Edition 41 (12), 2034–2057.
Lienhard, J.L., 2008. A Heat Transfer Textbook, third ed.. Phlogiston Press, Cambridge, Massachusetts.
Linton, J., 2000. Electronic products at their end-of-life: options and obstacles. Journal of Electronics Manufacturing 9 (1), 29–40.
Liu, Y., Gall, K., Dunn, M., Greenberg, A., Diani, J., 2006. Thermomechanics of shape memory polymers: uniaxial experiments and constitutive modeling. International Journal of Plasticity 22 (2), 279–313.
Liu, C., Qin, H., Mather, P.T., 2007. Review of progress in shape-memory polymers. Journal of Materials Chemistry 17 (16), 1543–1558.
Meng, Q., Hu, J., 2009. A review of shape memory polymer composites and blends. Composites Part A: Applied Science and Manufacturing 40 (11), 1661–1672.
Otsuka, K., Wayman, C., 1998. Shape Memory Materials. Cambridge University Press, Cambridge, UK.
Phadke, M., 1989. Quality Engineering using Robust Design. Prentice-Hall, Englewood Cliffs, New Jersey.
Sittner, P., Michaud, V., Schrooten, J., 2002. Modelling and material design of SMA polymer composites. Materials Transactions 43 (5), 984–993.
Suga T. Disassemblability Assessment for IM. First International Symposium on Environmentally Conscious Degign and Inverse Manufacturing, Proceedings. 1999:pp. 580–581.
Suga, T., Hosoda, N., 2000. Active Disassembly and Reversible Interconnection. IEEE International Symposium on Electronics and the Environment. 330–4.
Tandon, G.P., Goecke, K., Cable, K., Baur, J., 2009. Durability assessment of Styrene- and Epoxy-based Shape-memory polymer resins. Journal of Intelligent Material Systems and Structures 20 (17), 2127–2143.
CRG, 2009. Veriflex E2 Epoxy. http://crgindustries.com/veriflexE2.htm.
Willems, B., Dewulf, W., Duflou, J., 2005. Design for active disassembly (DfAD) an outline for future research. IEEE International Symposium on Electronics and the Environment. 129–34.
Willems, B., Dewulf, W., Duflou, J.R., 2007a. Active snap-fit development using topology optimization. International Journal of Production Research 45 (18–19), 4163–4187.
Willems, B., Dewulf, W., Duflou, J.R., 2007b. Pressure-Triggered Active Fasteners: Design results using Topology Optimization. 15th International Symposium on Electronics and the Environment (ISEE). Ieee, Orlando, FL. 184–189.
Zhang, H.C., Kuo, T.C., Lu, H., Huang, S.H., 1997. Environmentally conscious design and manufacturing: a State-of-the-Art Survey. Journal of Manufacturing Systems 16 (5), 352–371.